

Charge transfer in slow collisions of H^+ with Na

Anh-Thu Le,¹ Chien-Nan Liu,² and C. D. Lin¹

¹*Department of Physics, Cardwell Hall, Kansas State University, Manhattan, Kansas 66506, USA*

²*Institute of Physics, National Chiao-Tung University, Hsinchu 300, Taiwan*

(Received 26 March 2003; published 9 July 2003)

We reexamined charge-transfer cross sections for protons colliding with Na($3s$) atoms for collision energies from the threshold at 1.7 eV to 40 eV using the recently developed hyperspherical close-coupling method. Our results disagree with the recent calculations by Dutta *et al.* [Phys. Rev. A **63**, 022709 (2001)], but are in good agreement with the earlier calculations of Croft and Dickinson [J. Phys. B **29**, 57 (1996)] except at energies below 3 eV. Our calculations support the doubt on the experimental data of Kushawaha.

DOI: 10.1103/PhysRevA.68.012705

PACS number(s): 34.70.+e, 31.15.Ja

I. INTRODUCTION

Collisions involving sodium atoms and protons have been studied extensively in the last few decades. Most of the theoretical and experimental works have been focused on collisions at energies of the order of keV's. Despite its apparent simplicity, this collision system has generated a great deal of controversy. In the higher-energy region, the controversy has been more or less settled now, in that newer theoretical and experimental results for total charge-transfer cross sections are in good agreement [1–7]. Attention in the keV-energy region has recently been turned to differential cross sections and orientation parameters, including the recent experiments with laser-cooled Na targets [8]. In the low-energy region, from the threshold at 1.7 eV to, say, about 50 eV (all the collision energies in this paper refer to the center-of-mass energies), controversy still remains even for the total charge-transfer cross sections. Such cross sections are needed in order to understand the ionization distribution of stellar winds [9] and the interpretation of spectral distributions of the resonance line of sodium atoms [10]. Experimentally there exists only one measurement by Kushawaha [11]. This experimental result was first challenged by Croft and Dickinson who performed quantum-mechanical close-coupling calculations based on the molecular states of the collision complex [12]. They have used the so-called reaction coordinates [13,14] to account for electron translational effects. The total charge-transfer cross sections from the calculation by Croft and Dickinson showed rapid decrease as the collision energy drops below 10 eV, while the experimental data of Kushawaha gave a relatively constant cross section in this region. In a recent paper [15], Dutta *et al.* did a similar quantum-mechanical calculation with identical molecular basis except that the electron translational effect was introduced via atomic plane-wave-type translational factors. Their results show strong disagreement with those of Croft and Dickinson, but are in good agreement with the experimental data of Kushawaha.

In view of this controversy, we decided to examine the proton-sodium collision system using the recently developed hyperspherical close-coupling method (HSCC) [16]. The HSCC method is formulated similarly to the perturbed stationary states (PSS) approximation but without the well-known difficulties encountered in the PSS approach. Thus,

unlike the reaction coordinate method used by Croft and Dickinson or the electron translational factors used by Dutta *et al.*, no additional assumptions were needed beyond the truncation of the number of adiabatic channels included in the calculation. For proton-sodium collisions at low energies, only the valence electron of sodium is involved; thus we approximate the sodium as a one-electron atom in a core potential, with the model potential taken from Croft and Dickinson. We then solved the model collision system by expanding the total wave function in hyperspherical coordinates similar to that used in the PSS approach except that the hyper-radius is the adiabatic parameter. The HSCC method will be briefly reviewed in Sec. II.

From the present HSCC calculation, we were unable to reproduce the results of Dutta *et al.* We found good agreement with the results of Croft and Dickinson except at energies below 3 eV. The origin of these discrepancies will be discussed in Sec. III after our calculated results are presented. In Sec. IV we will conclude with comments on the different theoretical approaches for low-energy ion-atom collisions and the relation between the HSCC and traditional approaches.

II. THEORETICAL METHOD

To determine the electron-capture cross sections in ion-atom collisions, we use the hyperspherical close-coupling method where the hyperradial equations are solved using a combination of the R-matrix propagation and slow/smooth-variable discretization methods. The theory has been described in detail in Ref. [16]. We give here only a brief overview of the method.

The HSCC method has been developed for describing three-body collision systems so far. We approximate the proton-Na collision system as consisting of an electron in a Na^+ core and a proton. The effective potential of Na^+ was taken from Allan [17], which was also used by Croft and Dickinson. The three-body problem is then solved in the mass-weighted hyperspherical coordinates. In the “molecular” frame, the first Jacobi vector $\boldsymbol{\rho}_1$ is chosen to be the vector from Na^+ to H^+ , with reduced mass μ_1 ; and the second Jacobi vector $\boldsymbol{\rho}_2$ goes from the center of mass of Na^+ and H^+ to the electron, with reduced mass μ_2 . The hyper-radius R and hyperangle ϕ are defined as

$$R = \sqrt{\frac{\mu_1}{\mu} \rho_1^2 + \frac{\mu_2}{\mu} \rho_2^2}, \quad (1)$$

$$\tan \phi = \sqrt{\frac{\mu_2 \rho_2}{\mu_1 \rho_1}}, \quad (2)$$

where μ is arbitrary. Another angle θ is defined as the angle between the two Jacobi vectors. We choose μ to be equal to μ_1 . The hyperradius R is then very close to the internuclear distance.

After introducing the rescaled wave function

$$\Psi(R, \Omega, \hat{\omega}) = \psi(R, \Omega, \hat{\omega}) R^{3/2} \sin \phi \cos \phi, \quad (3)$$

the Schrödinger equation takes the form

$$\left(-\frac{1}{2} \frac{\partial}{\partial R} R^2 \frac{\partial}{\partial R} + \frac{15}{8} + H_{ad}(R, \Omega) - \mu R^2 E \right) \Psi(R, \Omega, \hat{\omega}) = 0, \quad (4)$$

where $\Omega \equiv \{\phi, \theta\}$ and $\hat{\omega}$ denotes the three Euler angles of the body-fixed frame axes with respect to the space-fixed frame. H_{ad} is the adiabatic Hamiltonian

$$H_{ad}(R, \Omega, \hat{\omega}) = \frac{\Lambda^2}{2} + \mu R^2 V(R, \Omega), \quad (5)$$

where Λ^2 is the square of the grand-angular-momentum operator and $V(R, \Omega)$ gives the total Coulomb interaction.

To solve Eq. (4), we expand the rescaled wave function in terms of the normalized and symmetrized rotation functions \bar{D} , and the body-frame adiabatic basis functions $\Phi_{\nu I}(R, \Omega)$,

$$\Psi(R, \Omega, \hat{\omega}) = \sum_{\nu} \sum_I F_{\nu I}(R) \Phi_{\nu I}(R, \Omega) \bar{D}_{IM_J}^J(\hat{\omega}), \quad (6)$$

where ν is the channel index, J is the total angular momentum, I is the absolute value of the projection of \mathbf{J} along the body-fixed z' axis, and M_J is the projection along the space-fixed z axis. To solve the hyperradial equations, we divide the hyperradial space into sectors. We then use a combination of the R -matrix propagation method [18] to propagate the R matrix from one sector to the next, and the slow/smooth-variable discretization method [19] within each sector. The R matrix is propagated to a large hyperradius (depending on the collision energy) where the solution is matched to the known asymptotic solutions to extract the scattering matrix. The electron-capture cross section for each partial wave J is then obtained from the calculated scattering matrix.

The method described above has to be carried out for each partial wave J until a converged cross section is reached. Using the numerical procedure introduced in Liu *et al.* [16], such calculations can be easily carried out for many partial

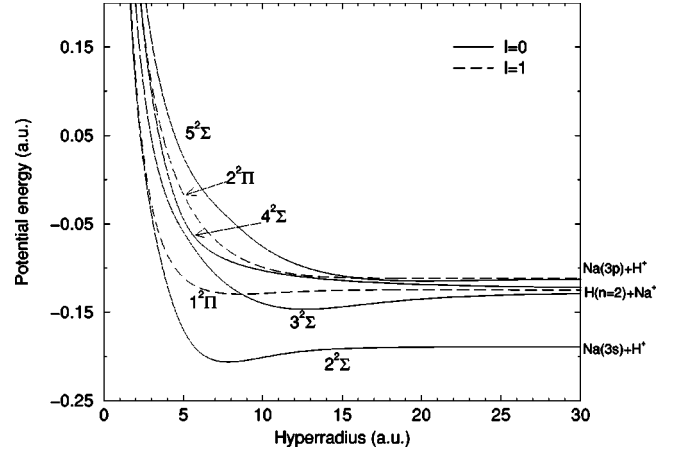
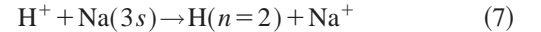


FIG. 1. Hyperspherical adiabatic potential curves for NaH^+ . The figure shows four $I=0$ channels in solid lines, two $I=1$ channels in broken lines.

waves. We have checked that the results are insensitive to the matching radius within the number of channels included in the calculation, see below.

III. RESULTS AND DISCUSSION

We are interested here in the determination of electron-capture cross section for the reaction



for collision energies from the threshold at 1.7 eV to 40 eV. To compare the present HSCC results with the calculations of Croft and Dickinson and of Dutta *et al.*, we used the same set of molecular basis (or hyperspherical channels) in the calculation. The adiabatic hyperspherical potentials included are shown in Fig. 1. Note that the curves are not molecular potential curves, but are rather hyperspherical potential curves. However, we have chosen the scaling mass such that

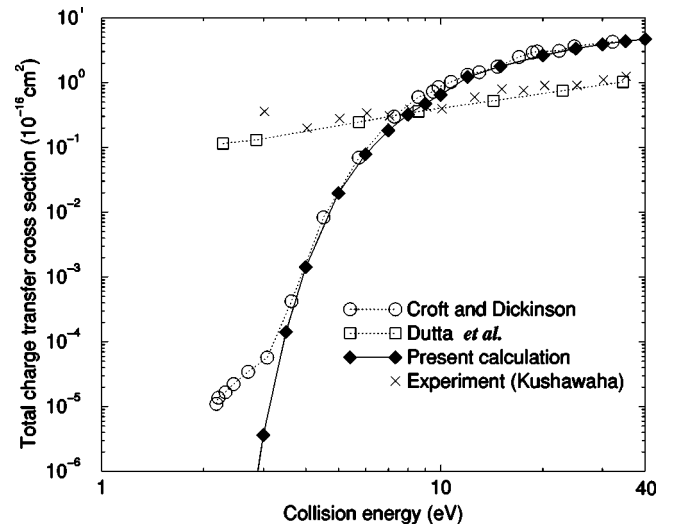


FIG. 2. Comparison of the total charge-transfer cross sections for $\text{H}^+ + \text{Na}(3s) \rightarrow \text{H}(n=2) + \text{Na}^+$ reactions.

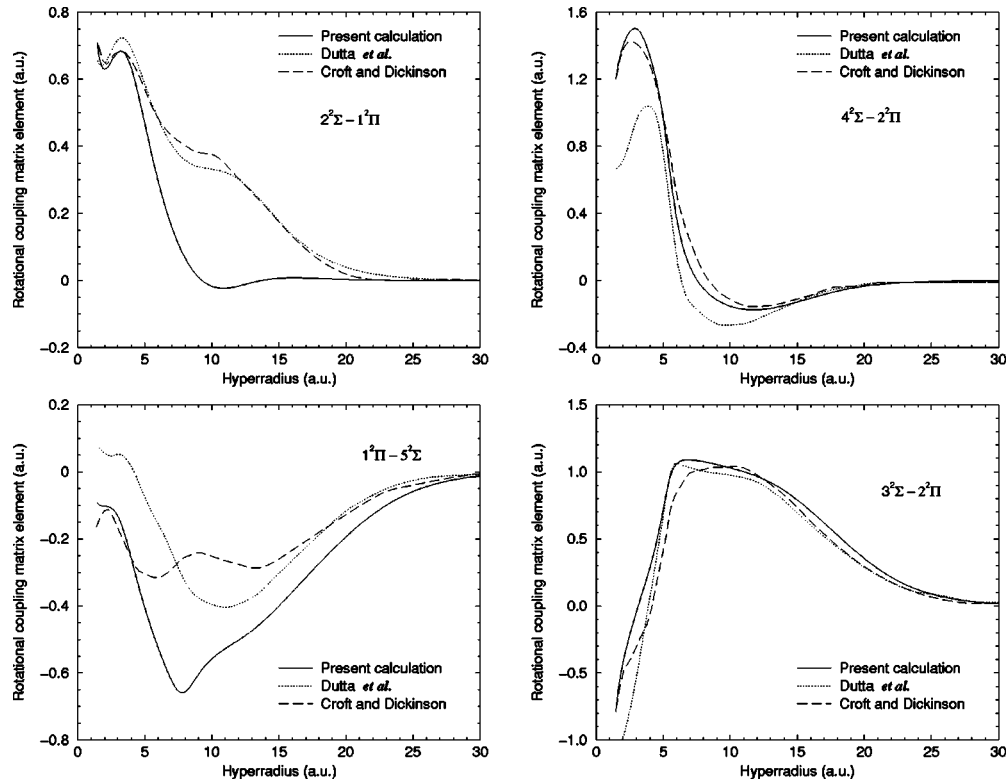


FIG. 3. Comparison of rotational coupling matrix elements from the three different calculations indicated in the figure. In the present calculation, we have chosen μ to be equal to μ_1 such that the hyperradius is essentially equal to the internuclear distance for $R > 0.1$ a.u.

the hyperradius is essentially equal to the internuclear separation except for distances less than around 0.1 a.u. Comparing Fig. 1 with the molecular potential curves, there are no apparent differences.

In Fig. 2 we show the total charge-transfer cross section [or equivalently total charge-transfer cross section to $H(n=2)$ states in this energy region] from the present HSCC calculation and compare it to the experimental data of Kushawaha, the calculations of Dutta *et al.*, and of Croft and Dickinson. Clearly ours do not agree with the experiment nor with the theoretical results of Dutta *et al.*, but agree well with the calculations of Croft and Dickinson except at energies below about 3 eV. In this low-energy region, our cross section drops rapidly while in Croft and Dickinson, the cross section shows a kink at about 3 eV.

What are the sources of the differences among the three theoretical calculations? To begin with, the potential curves from the three calculations are essentially identical. Thus we next compare the coupling matrix elements. The comparison of radial matrix elements is not possible since they are not shown in the papers of Croft and Dickinson, nor in the paper by Dutta *et al.* In the HSCC calculation, the radial coupling was not calculated, nor used. However, one can compare the rotational coupling matrix elements from the three different approaches. This is especially relevant for the present collision system since all three calculations agree that the $I=1$ channels are predominantly populated in the 3–40 eV region.

In Fig. 3 the rotational coupling matrix elements from the three calculations are shown. [The rotational coupling is

given as $C(R)/R^2$. Only $C(R)$ is shown in the figure following the general convention.] First we focus on the rotational coupling between the $1^2\Pi$ and the $2^2\Sigma$ (see Fig. 1) potential curves. The couplings from Croft and Dickinson and from Dutta *et al.* are in good agreement. (We have multiplied the data of Dutta *et al.* in their Fig. 3 by $\sqrt{2}$ to get the correct comparison.) This is not surprising since the two methods intrinsically are similar. The rotational coupling from the HSCC agrees well with these two calculations, especially in the region where it is important ($R < 5$ a.u.). Other rotational matrix elements in Fig. 3 also show reasonable agreement. But does the difference in the rotational coupling account for the discrepancy in the calculated total charge-transfer cross sections? By comparing our $I=1$ cross sections with those from Croft and Dickinson (not shown), we found good agreement over the whole energy range. In contrast, the $I=1$ component cross sections from Dutta *et al.* are much higher throughout the energy range. In fact, despite that all the three calculations were carried out using six channels as shown in Fig. 1, a two-channel calculation including only the $2^2\Sigma$ and $1^2\Pi$ channels can already produce nearly identical results. We replaced the rotational coupling matrix elements from our calculation by those from Dutta *et al.* and we were unable to reproduce their results. Instead the results remain close to what we obtained from the HSCC method.

We next discuss the difference in the total cross sections between the HSCC and those of Croft and Dickinson below 3 eV. As indicated above, for the $I=1$ channels, we have good agreement over the whole energy range. However, in

Croft and Dickinson, their $I=0$ cross sections to the $3^2\Sigma$ and $4^2\Sigma$ channels become dominant at energies below 3 eV. Thus the discrepancy between the present HSCC and that of Croft and Dickinson is due to the radial coupling for which we have not been able to make a direct comparison. In our calculation, cross sections for the $3^2\Sigma$ and $4^2\Sigma$ channels drop precipitously at low energies as for the $1^2\Pi$ channel and remain small in comparison to that channel.

By examining the potential curves in Fig. 1 we found that it is easier to interpret the results from the present calculation. At low energies, the radial coupling between $2^2\Sigma$ and $3^2\Sigma$ is not efficient for making direct transition from the $2^2\Sigma$ curve to the $3^2\Sigma$ curve despite the avoided crossing at about 12 a.u. since the energy gap is too large. An efficient mechanism for populating the excited states is via the rotational coupling. The electron will follow the $2^2\Sigma$ curve and gets promoted to a hyperradius (or internuclear separation) below 4 a.u. where the $2^2\Sigma$ curve and the $1^2\Pi$ curve are nearly degenerate. The rotational coupling between $2^2\Sigma$ and $1^2\Pi$ shown in Fig. 3 in this region would provide an effective mechanism in exciting the electron to the $1^2\Pi$ curve, thus populating the $I=1$ channels after the collision. As the collision energies decrease, the classical turning point for each partial wave will move further to larger R where the energy gap between the $2^2\Sigma$ curve and the $1^2\Pi$ curve becomes larger (see Fig. 1), thus the rotational coupling becomes inefficient and thus the $I=1$ charge-transfer cross section drops rapidly. At these low energies, there are no mechanisms that can efficiently populate the $3^2\Sigma$ and the $4^2\Sigma$ channels directly and any transition would have to go through the $1^2\Pi$ channel as the intermediate step. One may wonder if the $3^2\Sigma$ can be efficiently populated by the rotational coupling with the $1^2\Pi$ at the crossing near 9 a.u. However, this coupling can occur only after the $1^2\Pi$ channel is populated at smaller R , and thus should at most have the same energy dependence as the $1^2\Pi$ channel. Thus we do not expect the $I=0$ channel to become dominant at lower energies.

In Fig. 4 we show the impact-parameter-weighted charge-transfer probability vs impact parameter at selective collision energies. Note that in our calculation we never use the semiclassical concept. In comparing the partial-wave cross sections from the quantum calculation with the transition probabilities from the semiclassical calculation, we employ the relation

$$\sigma_J = \frac{2\pi b P(b)}{k}, \quad (8)$$

with $J=kb$, where k is the momentum. Except for 5 eV, we note that the cross section derives its contribution mostly from impact parameters below 3 a.u., clearly showing that the rotational coupling is the dominant mechanism for populating the charge-transfer channels in this energy region.

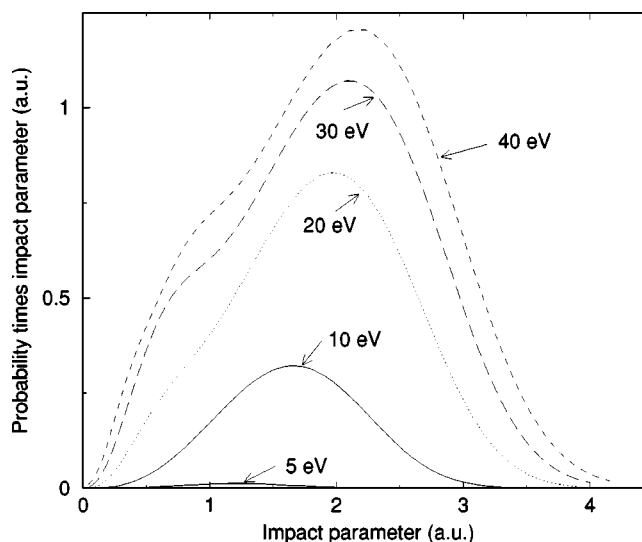


FIG. 4. Total charge-transfer transition probability times impact parameter as a function of impact parameter at selective collision energies.

IV. CONCLUSIONS

In this paper we used the hyperspherical close-coupling method (HSCC) to calculate electron-capture cross sections for the $H^+ + Na(3s) \rightarrow H(n=2) + Na^+$ reaction, from threshold at 1.7 eV to 40 eV. Our results agree with the earlier calculations of Croft and Dickinson except at energies below 3 eV. Our results do not agree with the recent calculations of Dutta *et al.* nor with the earlier experiment of Kushawaha. The HSCC calculations were carried out without the need of introducing somewhat *ad hoc* reaction coordinates or electron translational factors. On the other hand, a good agreement between the HSCC results and the reaction coordinate calculations of Croft and Dickinson indicates that charge-transfer cross sections are not very sensitive to the precise form of the switching function used in the reaction coordinate method. Still the remaining discrepancy at lower energies may be an indication of the limitation of the reaction coordinate approach. From the few collision systems we have examined so far, the discrepancy occurs only when the cross sections are small, as in the present case. In other words, despite of the somewhat *ad hoc* nature of the reaction coordinate method, it can be used to obtain reliable reaction cross sections at low energies.

ACKNOWLEDGMENTS

This work was supported in part by Chemical Sciences, Geosciences and Biosciences Division, Office of Basic Energy Sciences, Office of Science, U.S. Department of Energy. C.N.L. also acknowledges support from the National Science Council, Taiwan, under Grant No. NSC 91-2119-M-009-002. We also thank Dr. C. M. Dutta for communicating her results to us in an effort to resolve the source of the discrepancies.

- [1] C. Courbin, R.J. Allan, P. Salas, and P. Wahnon, *J. Phys. B* **23**, 3909 (1990).
- [2] W. Fritsch, *Phys. Rev. A* **30**, 1135 (1984).
- [3] R. Shingal and B.H. Bransden, *J. Phys. B* **20**, 4815 (1987).
- [4] A. Dubois, S.E. Nielsen, and J.P. Hansen, *J. Phys. B* **26**, 705 (1993).
- [5] F. Aumayr, G. Latikis, and H. Winter, *J. Phys. B* **20**, 2025 (1987).
- [6] T. Royer, D. Dowek, J.C. Houver, J. Pommier, and N. Andersen, *Z. Phys. D: At., Mol. Clusters* **10**, 45 (1988).
- [7] M. Gieler, F. Aumayr, P. Ziegelwanger, H. Winter, and W. Fritsch, *Phys. Rev. A* **43**, 127 (1991).
- [8] M. van der Poel, C.V. Nielsen, M.-A. Gearba, and N. Andersen, *Phys. Rev. Lett.* **87**, 123201 (2001).
- [9] A. Natta and C. Giovanardi, *Astrophys. J.* **356**, 646 (1990).
- [10] K. Watson and D.M. Meyer, *Astrophys. J. Lett.* **473**, L127 (1996).
- [11] V.H. Kushawaha, *Z. Phys. A* **313**, 155 (1983).
- [12] H. Croft and A.S. Dickinson, *J. Phys. B* **29**, 57 (1996).
- [13] W.R. Thorson and J.B. Delos, *Phys. Rev. A* **18**, 135 (1978).
- [14] J.B. Delos, *Rev. Mod. Phys.* **53**, 287 (1981).
- [15] C.M. Dutta, P. Nordlander, M. Kimura, and A. Dalgarno, *Phys. Rev. A* **63**, 022709 (2001).
- [16] Chien-Nan Liu, Anh-Thu Le, Toru Morishita, B. D. Esry, and C. D. Lin, *Phys. Rev. A* **67**, 052705 (2003).
- [17] R.J. Allan, *J. Phys. B* **19**, 321 (1986).
- [18] K.L. Baluja, P.G. Burke, and L.A. Morgan, *Comput. Phys. Commun.* **27**, 299 (1982).
- [19] O.I. Tolstikhin, S. Watanabe, and M. Matsuzawa, *J. Phys. B* **29**, L389 (1996).